Assessment of magnetic nanodroplets propagation in porous media via effluent analysis

Seyedeh Hannaneh Ahmadi[1, *], *Boxin Ding*[2], *Seyed Emad Siadatifar*[1], *Steven Bryant*[1,4], *and Apostolos Kantzas*[1,3]

[1] Department of Chemical and Petroleum Engineering, University of Calgary, Calgary, AB Canada T2N 1N4

[2] School of Advanced Materials, Peking University, Shenzhen Graduate School, Shenzhen, China 518055

[3] PERM Inc. TIPM Laboratory, Calgary, AB Canada T2E 6P2

[4] Canada Excellence Research Chair in Materials Engineering for Unconventional Oil Reservoirs, Canada

Abstract. In recent years, there has been a growing interest in using nano-colloidal dispersions like nanofluids, nanoemulsions, and nanofoams for subsurface applications due to their reactivity and large surface area. Pickering nanoemulsions, stabilized by nanoparticles, are particularly promising for subsurface use because of their stability. This research begins by synthesizing different ratios of polymer shell to iron oxide (Fe_3O_4) nanoparticle core (4:1, 2:1, and 0.5:1) to form stable oil-in-water (O/W) nanoemulsions. Then, core flooding experiments are performed in a sandpack to mimic subsurface conditions, evaluating nanoemulsion transport and retention. The aim is to apply these nanoemulsions for fracture characterization, with the sandpack replicating proppant-filled fractures. Various experiments, including Dynamic Light Scattering (DLS), Inductively Coupled Plasma Spectrometry (ICP), Magnetic Susceptibility, and Pressure Drop (DP) analyzed nanoemulsion behavior during flooding. Furthermore, X-ray CT scanning during nanoemulsion and chase water flooding quantitatively monitored the nanoemulsion flow patterns. Results indicate that a 4:1 polymer-to-nanoparticle ratio provides the most stable nanoemulsion, easily transported through the sandpack with minimal retention. Pressure drop results show increased pressure during nanoemulsion flooding due to higher viscosity, but lower pressure drop during chase water flooding, suggesting reduced retention at optimal coating ratios. Overall, the study highlights the potential of Pickering nanoemulsions for subsurface applications like hydraulic fracturing, as long as their stability and transport features are confirmed.

1 Introduction

The encapsulation of nanomaterials within oil-in-water (O/W) emulsions, known as Pickering emulsions, has emerged as a promising strategy for subsurface remediation in recent decades. This innovative approach aims to mitigate the aggregation and deposition of nanomaterials by employing a two-fold strategy. Firstly, it involves reducing the size of the droplets to the nanoscale. By breaking down the droplets into much smaller units, the surface area-to-volume ratio increases significantly, which assists in minimizing the likelihood of nanomaterial aggregation. This reduction in droplet size also enhances the dispersion of nanomaterials within the emulsion, ensuring more uniform distribution and improved accessibility to the target subsurface environment [1]. Secondly, the approach relies on the exclusive use of solid nanoparticles to stabilize the nanoscale droplets. These nanoparticles are uniquely capable of adhering to the oil-water interfaces of the emulsion droplets by applying energy to the system. This attachment effectively forms a protective layer around the droplets, shielding them from coalescence and aggregation [2]. Moreover, the presence of these solid nanoparticles imparts additional stability to the emulsion system by reinforcing the steric barrier at the interface between the oil and water phases. By combining these two elements – droplet size reduction and solid nanoparticle stabilization – the approach offers a comprehensive solution to the challenge of mitigating nanomaterial aggregation and deposition. It represents a sophisticated yet practical strategy for ensuring the efficient delivery and dispersion of nanomaterials in subsurface applications, with the potential to significantly enhance the effectiveness of environmental amendments in contaminated environments or other applications in oil and gas industry comprising fracture characterization or enhanced oil recovery (EOR) strategy [3].

Meanwhile, this novel method presents several advantages over traditional approaches for subsurface applications. Firstly, Pickering nanodroplets offer improved delivery of oil amendments without encountering the retention and injectivity challenges often

* Corresponding author: seyedehhannaneh.ahma@ucalgary.ca

associated with larger droplets in rocks and fine-grain sediments. Secondly, by attaching nanomaterials to nanodroplets, we can facilitate delivery without the complexities and costs associated with ensuring the stable dispersion of non-aggregating nanomaterials. Lastly, the synergistic effects of environmental remediation can be achieved by combining nanomaterials to catalyze the chemical degradation of contaminants with oil to promote microbial degradation. This highlights the potential of Pickering nanodroplets as a versatile and efficient means of delivering environmental amendments for subsurface remediation. The robust stability and enhanced functionality offered by this approach confirm its potential for addressing complex environmental challenges in a sustainable manner [4,5].

Pickering nanoemulsions incorporating iron or iron oxide nanoparticles present a promising alternative for subsurface application particularly evaluating fractures through flowback analysis in tight reservoirs. These nanoemulsions possess advantageous features such as superparamagnetic properties for in-situ detection, simple synthesis methods, customizable size, robust stability, minimal retention in fractures, and eco-friendly characteristics. Nevertheless, the effective application of these magnetic nanodroplets for fracture characterization requires addressing concerns related to their long-term stability and transport behavior [6,7]. This is due to the potential aggregation and deposition of nano-dispersed fluids on solid surfaces within porous media, which can diminish the concentration of nano-colloidal dispersions in the bulk fluid. Consequently, this can lead to a significant decrease in transportation efficiency and result in notable resistance and clogging in microchannels [8]. However, evaluating the flow dynamics of these fluids becomes more complicated in concentrated systems due to hydrodynamic interactions among droplets, potentially inducing coalescence phenomena, and interactions between pore walls and droplets [9,10].

Several factors contribute to this complexity:

i) Enhanced droplet deformation and self-diffusion, predominantly in the velocity direction compared to the vorticity direction.

ii) Effects of droplet confinement.

iii) Shear-induced diffusion, leading to droplet movement away from regions of higher concentration.

iv) Influence of matrix viscoelasticity, influenced by normal stresses, impacting droplet migration towards the pore centerline [11,12].

Physicochemical properties such as size, shape, and surface charge influence how nanoemulsions interact with porous media. For instance, smaller droplet sizes may facilitate easier passage through pore throats, while irregular shapes could lead to entrapment. Additionally, the chemical composition of nanoemulsions and their surrounding solution affects their behavior; for example, pH and ionic strength can alter the stability of the emulsion. Furthermore, the presence of natural organic matter in the environment can impact interactions between nanoparticles and the porous medium. The hydrodynamic conditions during injection, such as flow rate and pressure, also play a crucial role. High flow rates may enhance dispersion, while increased pressure can force nanoemulsions deeper into the porous medium. Despite the extensive research on conventional nanoemulsions, there is a gap in understanding the transportation behavior of Pickering nanoemulsions in porous media [13].

McAuliffe (1973) investigated the displacement characteristics of emulsions with varying droplet sizes under consistent pressure conditions. Their study highlighted the flow behavior of diluted oil-in-water (O/W) emulsions, generated from the interaction of acidic crude oil with a caustic solution, within porous consolidated Berea sandstone. They noted a significant reduction in permeability, sometimes up to 90%, due to the flow of these emulsions. This reduction was particularly pronounced for larger droplet sizes, attributed to droplet entrapment within pores, adherence to pore walls, and overall medium clogging. The study emphasized the necessity to overcome capillary resistance within pore throats for oil droplet deformation [14]. McAuliffe's observations indicated that the injection force exceeded the capillary resistance, as discussed in Bulletin 1933 [15]. Long Yu et al. [16] conducted a series of sandpack flow experiments aimed at investigating the efficacy of heavy oil-in-water (O/W) emulsions in causing plugging. They utilized a formulation consisting of 0.1 wt.% Span 60, 0.1 wt.% Tween 80 as surfactants, and 0.025 wt.% NaOH. Their experiments demonstrated that the heavy O/W emulsions led to significant reductions in permeability, with plugging effectiveness more than 99% in sandpacks. The degree of permeability reduction was found to be heavily influenced by several factors. Notably, increasing the concentration of oil in the emulsion and the volume of injected emulsion slugs resulted in more pronounced permeability reductions. Conversely, higher sandpack permeability and injection flow rates were associated with diminished permeability reduction due to emulsion plugging.

The primary objective of this study was to synthesize polymer-coated iron oxide nanoparticles with varying thicknesses of polymer shell coating on Fe_3O_4 nanoparticle cores, specifically in ratios of 4:1, 2:1, and 0.5:1. Subsequently, Pickering nanoemulsions were prepared by incorporating these synthesized nanoparticles, which were anchored onto the surface of oil droplets, enhancing their dispersal within the water phase. To comprehensively understand the retention and displacement behavior of these newly synthesized Pickering nanoemulsions, a series of systematic core flooding experiments were conducted using a sandpack.

Several experimental techniques were employed to analyze the behavior of nanoemulsions during flooding. These techniques include:

Dynamic Light Scattering (DLS via a NanoPlus HD Particle Size & Zeta Potential Analyzer): DLS is used to measure the size distribution of nanoparticles or droplets in the nanoemulsion. By analyzing the intensity of scattered light, DLS provides information about the hydrodynamic diameter of the particles, helping to characterize the stability and dispersity of the nanoemulsion.

Inductively Coupled Plasma Spectrometry (ICP via 8900 ICP-QQQ): ICP is a technique used to quantify the

concentration of specific elements, such as iron in the case of iron oxide nanoparticles. In this case it is possible to track the presence and distribution of nanoparticles within the nanoemulsion and during flooding experiments.

Magnetic Susceptibility (via Bartington MS2C sensor): Magnetic susceptibility measurements are employed to assess the distribution and mobility of magnetic nanoparticles, such as iron oxide nanoparticles, within the nanoemulsion and porous media.

Pressure Drop Analysis: Pressure drop measurements are performed to evaluate the resistance to flow encountered by the nanoemulsion as it passes through the porous media during flooding experiments. By monitoring changes in pressure, we can assess the efficiency of displacement and retention of the nanoemulsion within the porous medium.

X-ray Computed Tomography (CT): To obtain detailed spatial and temporal profiles of the nanoemulsion transport and retention within the porous media, X-ray computed tomography (CT) imaging was utilized. A GE Lightspeed full-body scanner was employed for this purpose. This advanced imaging technique enabled the measurement of density profiles within the sandpacks used in the experiments. X-ray CT imaging provided high-resolution images allowing for precise visualization of the distribution and movement of the nanoemulsions. By capturing the density variations, it was possible to track the location and concentration of the nanodroplets as they moved through the porous medium. This non-invasive technique offered a significant advantage in observing the in-situ behavior of the nanoemulsions without disturbing the system.

These experimental techniques collectively provide valuable information about various aspects of nanoemulsion behavior during flooding, including particle size distribution, particle distribution and retention in porous media.

The experiments were run continuously. In the first day the displacement and CT scanning, were conducted. In the next day DLS, susceptibility, and ICP were measured. The waiting time was around 9-12 hours. Effluent was collected in different tubes for each 0.2 PV.

2 Experimental procedures

2.1 Materials

In this study, n-dodecane ($C_{12}H_{26}$), with a density of 0.75 g/cm^3 and a molecular weight (Mw) of 170.33 g/mol at 99% purity from Sigma-Aldrich, was dispersed in Milli-Q water. Engineered iron oxide nanoparticles (IONP NPs) served as emulsifiers for synthesizing Pickering nanoemulsions. Bare IONPs (Fe_3O_4 NPs) were provided from US Research Nanomaterials Inc., with a diameter range of 20-30 nm, specific surface area of 40-60 m^2/g, purity >99%, and true density of 4.8-5.1 g/cm^3. Poly(4-styrenesulfonic acid-co-maleic acid) sodium salt-20 kD (PSS-co-MA) from Sigma-Aldrich coated the bare NPs. hydrochloric acid (HCl, 37%, Mw: 36.46 g/mol) and sodium hydroxide (NaOH, >98%, Mw: 40 g/mol) from Fisher Chemical were used to adjust the aqueous phase's pH.

2.2 Synthesis of Pickering nanoemulsion via iron oxide nanoparticles (IONP) modification method

Initially, in the primary stage of the process, magnetic bare iron oxide nanoparticles underwent a functionalization process with a polymer to enhance their properties related to hydrophilicity, dispersibility, and emulsification capacity. To regulate the thickness of the polymer layer encompassing the nanoparticles, varying polymer-to-nanoparticle ratios were employed. These ratios, including 4:1, 2:1, and 0.5:1, represented different weight percentages of polymer to nanoparticles. For instance, in one scenario, a mixture of 4wt% PSS-co-MA polymer and 1wt% IONPs were individually dissolved in 500 mL of DI water, with the pH adjusted to 5. Subsequently, a homogenizer (VWR 250, VWR Scientific Inc., USA) was utilized to agitate the aqueous solutions for 10 minutes at a rotation speed of 12,000 rpm, facilitating powder solubility in water.

Following the achievement of uniform solutions devoid of visible polymer and particle presence, the polymeric nanofluids underwent 60 minutes of ultrasonication using a probe sonicator set at a pulse on/off time of 30 s/30 s and an amplitude of 50%, conducted within an iced water bath. This ultrasonication process promoted the effective attachment of PSS-co-MA polymer molecules onto the IONPs' surface, forming a polymer coating surrounding the core of the IONPs [17]. Subsequent to this, centrifugation of the polymeric nanofluids at 4000 RPM for 20 minutes was performed to separate any non-coated IONPs or residual PSS-co-MA polymers in the bulk fluid. The supernatant was then subjected to a concentration and washing process [18] using DI water in 100 kDa centrifugal filter tubes (AmiconUltra-12, 100 kDa, MilliporeSigma) for three consecutive centrifugation cycles, each lasting 30 minutes at a speed of 4000 RPM. Subsequently, an analysis utilizing inductively coupled plasma-mass spectrometry (ICP-MS) was conducted to determine the composition of the polymer-coated iron oxide nanoparticles (PIONPs), allowing assessment of the weight percentages of Fe and S in the concentrated nanofluids. The results revealed that the ratios of polymer coating to bare IONPs were 3.8, 1.9, and 0.7 for the mixtures of 4:1, 2:1, and 0.5:1 polymer-to-nanoparticle ratios, respectively.

In the second stage, the primary method for generating nanoemulsions involves reducing the size of dispersed droplets or disrupting the interface between phases through agitation or mechanical action to enhance the uniform dispersion of one phase within another [19]. After synthesizing polymer-coated iron oxide

nanoparticles (PIONPs) with various polymer-to-nanoparticle ratios (4:1, 2:1, and 0.5:1), three distinct Pickering nanoemulsions were fabricated. These nanoemulsions consisted of 1 wt.% PIONPs and 10 v/v% n-dodecane as an oil phase mixed with deionized water to a total volume of 100 mL, aiming to study how the thickness of the coating influences the displacement behavior of the nanoemulsions in porous media.

Initially, the entire solution underwent homogenization for 10 minutes at a rotation speed of 12,000 rpm. To tackle the issue of providing large oil droplet size with homogenizer, the homogenized solutions underwent sonication for 60 minutes with a pulse on/off time of 30 s/30 s and an amplitude of 50%. This step applied significantly higher energy (approximately 48 kJ) to achieve a more appropriate oil-water interface area and notably reduce the oil droplet size to the nanoscale. Subsequently, the freshly prepared Pickering nanoemulsions were immediately injected into the sandpack to evaluate their behavior regarding retention and displacement within porous media.

2.3 Sandpack preparation and Pickering nanoemulsion displacement evaluation in porous media

The sandpack configuration in this study included two end caps, two pieces of 300-mesh screen welded to prevent sand leakage, and two rubber stoppers for tight sealing. Fabricated from PVC to facilitate CT scan measurements, the sandpack holder measured 15 cm in length and 2.5 cm in internal diameter. This setup aimed to investigate how varying polymer-to-nanoparticle ratios affected the plugging ability and flow behavior of Pickering nanoemulsions. To ensure uniform packing, each sandpack was filled with a combination of fresh silica sand comprising 50% vol. of 50-70 mesh and 50% vol. of 70-100 mesh. Permeability adjustments were made by arranging sand mesh sizes and tightening the sandpack appropriately. Air removal from the sandpack involved vacuum suction for 30 minutes followed by carbon dioxide (CO_2) injection for 15 minutes. Vacuum suction was performed again to completely evacuate the air from the sandpack. Subsequently, deionized (DI) water containing 2 wt.% potassium iodide (KI) was imbibed into the sandpack for full saturation [20]. KI was added to the water phase to enhance contrast for CT scanning. Porosity and permeability were determined using material balance and Darcy's law, respectively. Operational parameters for drainage experiments are detailed in Table 1, including porosity (ϕ), permeability (k), pore volume (PV), and nanoemulsion and water injection flow rate (Q).

Table 1. Evaluated sandpack parameters.

Test #	Polymer -to-NP Ratio	Ø (%)	k (mD)	PV (mL)	Q (mL/min)
1.	0.5:1	44.1	4212.1	22.7	0.5
2.	2:1	38.6	3849.0	23	0.5
3.	4:1	38.4	5914.6	22.9	0.5

The experimental setup for core flooding tests depicted in Figure 1 comprises various instruments, including a syringe pump (model 500D, Teledyne ISCO, Lincoln, NE, USA), two vessels for deionized water and nanoemulsion, a pressure transducer (model PX409, OMEGA Engineering Inc., Stanford, CT, USA) capable of measuring pressure drop within the sandpack, a fully water-saturated sandpack, a computed tomography (CT) scanner, an in-line densitometer (model DMA HPM, Anton Paar) for effluent density measurement, and an effluent fraction collector (Foxy® R1, Teledyne ISCO). The experiments involved injecting 2 pore volumes (PV) of synthesized nanoemulsions into a horizontal sandpack followed by water flooding up to 5 PV at a constant flow rate of 0.5 ml/min. Effluents were collected periodically using the effluent fraction collector. Pressure drop was continuously recorded using the pressure transducer throughout the experiment. Nanoemulsion propagation assessed within the sandpack through Dynamic Light Scattering (DLS), Inductively Coupled Plasma Spectrometry (ICP), and Magnetic Susceptibility of effluent samples.

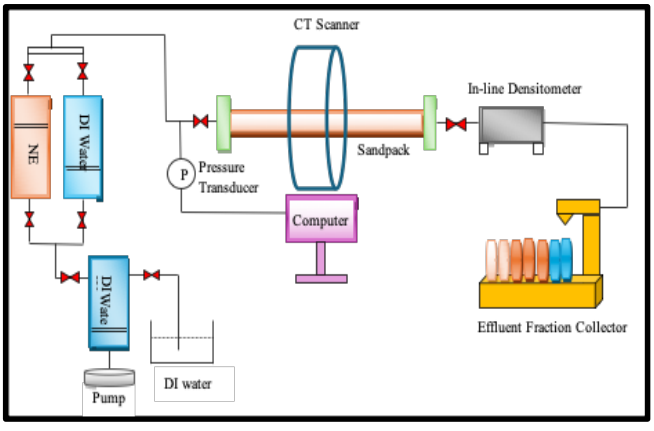

Fig. 1. Schematic diagram of the nanoemulsion displacement experiment.

3 Results and discussion

In this section, we explore the impact of different ratios of polymer shell coating to Fe_3O_4 nanoparticle core (specifically, 4:1, 2:1, and 0.5:1) on the stability and displacement behavior of synthesized nanoemulsions within porous media through effluent analysis. We assess

nanodroplets propagation in sandpack by investigating the size distribution of nanodroplets via DLS and measure pressure drops across the sandpack throughout the flooding procedure. The concentration of nanoparticles in effluent samples is evaluated along with measuring susceptibility property of effluents to characterize the stability and dispersity of the nanoemulsion within porous media. These parameters collectively aid in identifying the most efficient nanoemulsion formulation with the least retention in porous media. We provide a detailed discussion of these findings in this segment.

3.1 Effect of nanoemulsion displacement on pressure drop across the sandpack

Figures 2, 3, and 4 depict the pressure drop observed during nanoemulsion flooding, followed by water flooding, at respective polymer-to-nanoparticle ratios of 0.5:1, 2:1, and 4:1. In all experiments, the pressure drop enhances during NE flooding. The increased pressure drop during NE flooding can be attributed to two main factors: drag force and viscous force.

Drag Force: As the Pickering nanoemulsion flows through the pores, it interacts with the walls of the pore spaces. This interaction creates a drag force, which is essentially the frictional force between the fluid and the surface of the pores. Because nanoemulsions have a higher viscosity than water, they experience greater drag force as they flow through the porous medium, leading to a higher pressure drop.

Viscous Force: Viscous force is the internal resistance within the fluid itself as it flows. Higher viscosity fluids experience greater viscous force, which contributes to a higher pressure drop. In the case of Pickering nanoemulsions, their higher viscosity results in stronger internal friction between the fluid layers as they flow, leading to increased viscous force and consequently a higher pressure drop [21].

So, the combination of these drag and viscous forces results in a higher pressure drop during NE flooding compared to water flooding. However, the rate of pressure rise is notably more pronounced at the 2:1 and 0.5:1 ratio compared to the 4:1 ratio. Subsequently, during water flooding, the pressure drop diminishes and stabilizes as water displaces the nanoemulsion at all polymer-to-nanoparticle ratios. Conversely, at the 0.5:1 ratio, fluctuations in pressure drop emerge after 4 pore volumes of water injection. Moreover, the stabilized pressure drop at the 0.5:1 and 2:1 ratio is approximately double that of the 4:1 ratio, potentially attributable to enhanced nanoemulsion retention at lower polymer-to-nanoparticle ratios, thus hindering water's displacement. As a result, low polymer coating ratios on magnetic nanoparticles can lead to insufficient steric and electrostatic stabilization, increased aggregation, larger droplet sizes, and enhanced adsorption onto porous media surfaces. These factors collectively contribute to enhanced retention and instability of the nanoemulsion. Higher pressure drop during water flooding in the experiment with the coating ratio of 2:1 compared to 0.5:1 is related to lower permeability of the sandpack during the experiment. Consequently, at the coating ratio of 0.5:1, water redistributes its path, causing a progressive increase in pressure drop until it overcomes the capillary resistance of trapped nanoemulsions. This continuous process of water displacing trapped nanoemulsion leads to fluctuations in pressure drop at the mentioned ratio, contrasting with the more stable displacement observed at the 4:1 ratio. In this meanwhile, some properties of nanoemulsions were measured. The viscosity of nanoemulsions with different polymer-to-nanoparticle ratios was determined using a Brookfield Viscometer (Model DV2TLV Pro Extra). At the same time, the densities of all samples were evaluated utilizing a densitometer instrument (model DMA HPM, Anton Paar). The estimated parameters are shown in Table 2.

Table 2. Evaluated nanoemulsions properties.

Type of Nanoemulsion	Viscosity (cP)	Density (kg/m^3)
1. 0.5:1 (polymer-to-nanoparticle ratio)	2.16	0.994
2. 2:1 (polymer-to-nanoparticle ratio)	2.39	0.984
3. 4:1 (polymer-to-nanoparticle ratio)	2.35	0.945

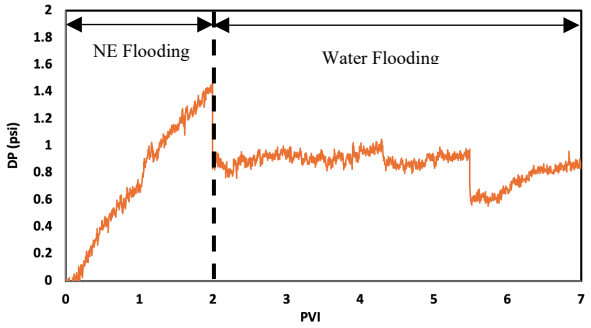

Fig. 2. The pressure drop pattern during NE flooding succeeded by water flooding at 0.5:1 polymer-to-nanoparticle ratio.

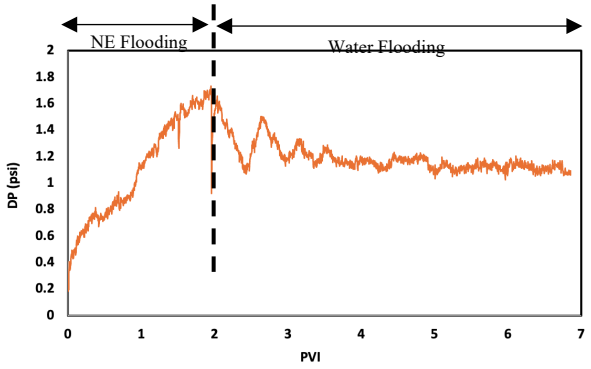

Fig. 3. The pressure drop pattern during NE flooding succeeded by water flooding at 2:1 polymer-to-nanoparticle ratio.

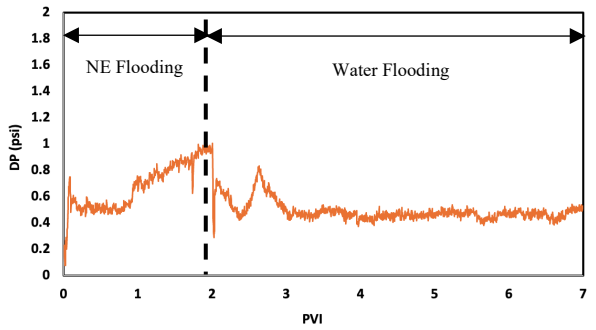

Fig. 4. The pressure drop pattern during NE flooding succeeded by water flooding at 4:1 polymer-to-nanoparticle ratio.

3.2 Effluent analysis of the flow tests

To further explore the transport and retention behaviour of the PIONP stabilized nanoemulsions in porous media, the effluents from the sandpack were collected and analyzed through DLS, ICP, and Susceptibility methods.

3.2.1 Effluents droplet size distribution during nanoemulsion and water flooding

Figures 5, 6, and 7 illustrate the distribution of effluent median droplet size over pore volume (PV) in various flow tests involving the injection of nanoemulsions with different polymer-to-nanoparticle ratios of 0.5:1, 2:1, and 4:1, respectively. The reference line denoted by a black dashed line represents the D50 of the injected nanoemulsion within the sandpack. Based on the pressure drop results observed during nanoemulsion and water flooding experiments, it is noted that the retention of PIONP-stabilized nanoemulsions becomes significant as the ratio of coated polymer on the nanoparticle shell decreases from 4:1 to 0.5:1. It is evident from Figures 5, 6, and 7 that the decrease in median droplet size in the effluent as retention becomes more prominent confirms the impact of polymer-to-nanoparticle ratio on nanoemulsion stability and transport in porous media. At lower coating ratios (0.5:1), where retention is significant, the observed decrease in droplet size suggests that larger droplets are preferentially retained within the sandpack, while smaller droplets are more likely to pass through. Conversely, at higher coating ratios (4:1), minimal retention leads to larger droplet sizes in the effluent, indicating less obstruction and clogging within the sandpack. In instances where there is minimal or no retention of nanoemulsion, D50 value is substantially higher than the injected reference value. As more fluid is produced during water flooding (after 3 PV), the majority of the effluent samples exhibit sizes smaller than their injected median reference size suggesting the presence of numerous small nanodroplets and dispersed nanoparticles in the water stream. However, this reduction in droplet size is the lowest at the polymer-to-nanoparticle ratio of 4:1, indicating minimal retention without considerable clogging in the sandpack. On the other hand, a notable difference in effluent droplet size occurs when the coating ratio diminishes to 0.5:1 which depicts that only small droplets can penetrate through the pores and come out of the sandpack.

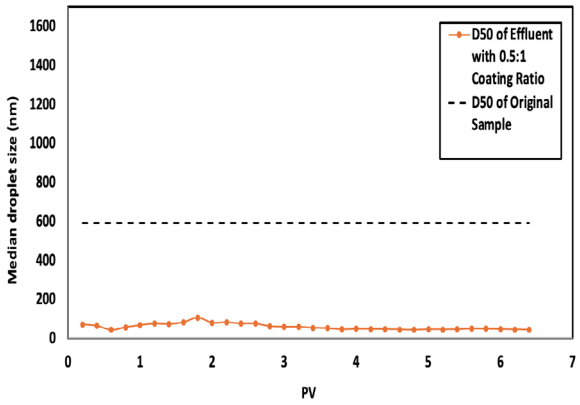

Fig. 5. Effluent droplet size as a function of PV for the flow test by injection of nanoemulsions with 0.5:1 polymer-to-nanoparticle ratio.

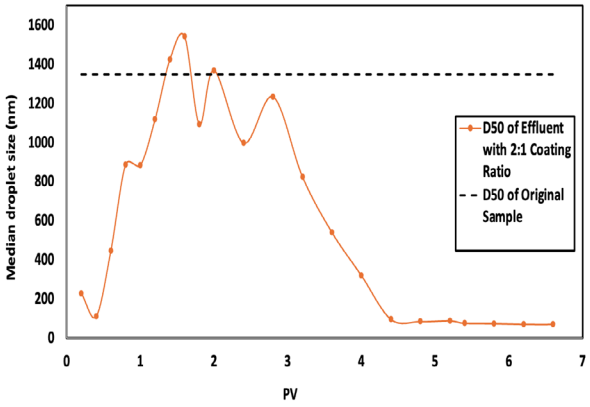

Fig. 6. Effluent droplet size as a function of PV for the flow test by injection of nanoemulsions with 2:1 polymer-to-nanoparticle ratio.

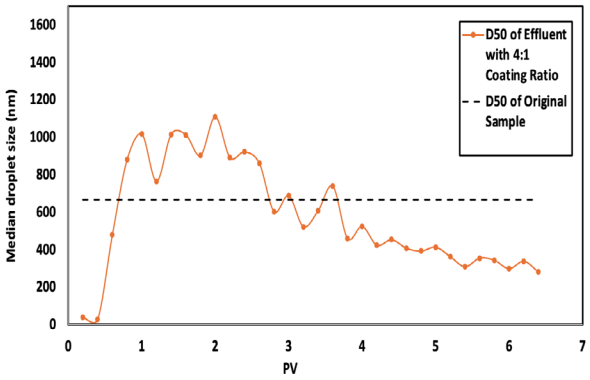

Fig. 7. Effluent droplet size as a function of PV for the flow test by injection of nanoemulsions with 4:1 polymer-to-nanoparticle ratio.

3.2.2 Effluents concentration profile during nanoemulsion and water flooding

Figures 8, 9, and 10 depict the results of ICP analysis conducted on effluents versus pore volume (PV) in three distinct flow tests. These tests involved the injection of nanoemulsions with different polymer-to-nanoparticle ratios of 0.5:1, 2:1, and 4:1, respectively. Nanoemulsion flooding was performed up to 2 PV, followed by chase water flooding up to 5 PV in each test. Subsequently, effluent samples were collected at intervals of 0.2 PV. The concentration is normalized as c/c_0, where c represents the effluent concentration and c_0 denotes the injectant concentration. In Figures 8, 9, and 10, the black lines illustrate the baseline concentration of the injected nanoemulsion within the sandpack. As can be seen, the normalized concentration of produced PIONP initially increases to approach the baseline concentration of the injected nanoemulsion, then decreases until no PIONP is observed in the effluents during NE and water flooding. However, throughout the analysis, as the ratio of polymer to nanoparticle diminishes, the concentration of effluents is lower than the baseline concentration indicating polymer coating detachment from PIONP and some IONP deposition in the porous media. As a result, greater retention of nanoemulsion occurs during displacement experiment by nanoemulsion with the polymer-to-nanoparticle ratio of 0.5:1. In contrast, the overlapping of the effluent concentration with the baseline indicates sufficient stability of the nanoemulsion at the 4:1 ratio, with minimal retention.

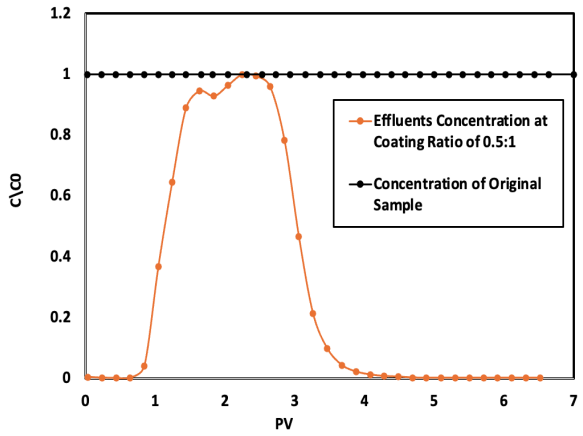

Fig. 8. ICP analysis of the effluents as a function of PV for the flow test by injection of nanoemulsions with 0.5:1 polymer-to-nanoparticle ratio.

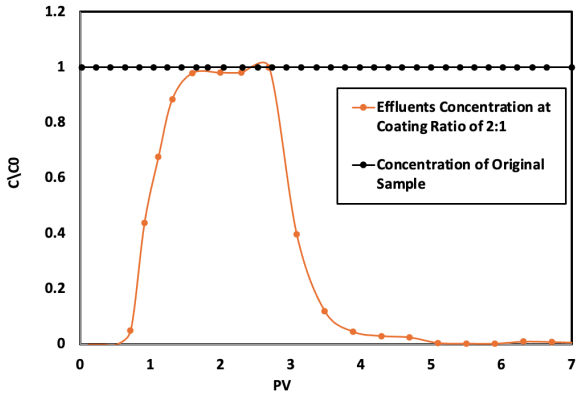

Fig. 9. ICP analysis of the effluents as a function of PV for the flow test by injection of nanoemulsions with 2:1 polymer-to-nanoparticle ratio.

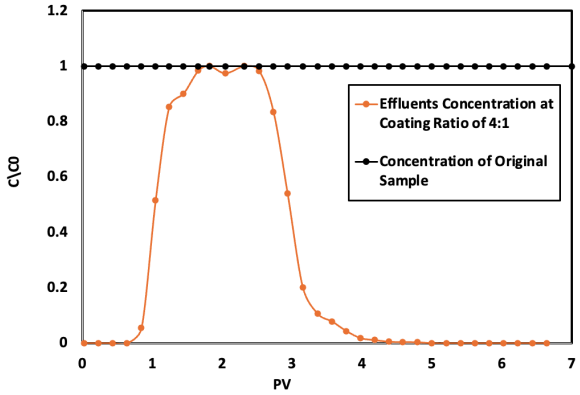

Fig. 10. ICP analysis of the effluents as a function of PV for the flow test by injection of nanoemulsions with 4:1 polymer-to-nanoparticle ratio.

3.2.3 Effluents susceptibility profile during nanoemulsion and water flooding

Figures 11, 12, and 13 present the results of susceptibility measurements conducted on effluents plotted against pore volume (PV) in three distinct flow experiments. These experiments involved nanoemulsions with varying polymer-to-nanoparticle ratios of 0.5:1, 2:1, and 4:1, respectively. Normalized susceptibility is defined as the effluent susceptibility divided by the injectant susceptibility. Similar to previous experiments, the black lines in Figures 11, 12, and 13 represent the baseline susceptibility of the injected nanoemulsion within the sandpack. It is evident that susceptibility measurements are verified by ICP analysis, as they exhibit similar trends. Upon injecting nanoemulsion into the sandpack, the normalized susceptibility of produced PIONP begins to increase after 0.8 PV, indicating the breakthrough of nanoemulsion. Subsequently, this property reaches the normalized susceptibility of the original sample, demonstrating the stability of nanoemulsion during the flooding experiment. After 2.8 PV, it diminishes to align with the zero line, indicating no more PIONP in effluents. This experiment illustrates that the synthesized Pickering

nanoemulsion can displace in porous media without any retention or deposition.

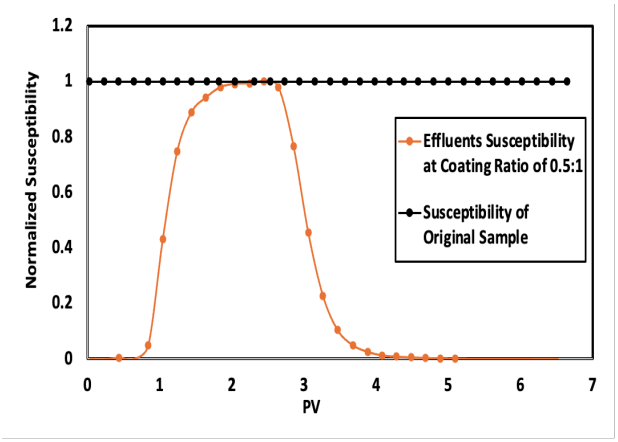

Fig. 11. Normalized susceptibility of the effluents as a function of PV for the flow test by injection of nanoemulsions with 0.5:1 polymer-to-nanoparticle ratio.

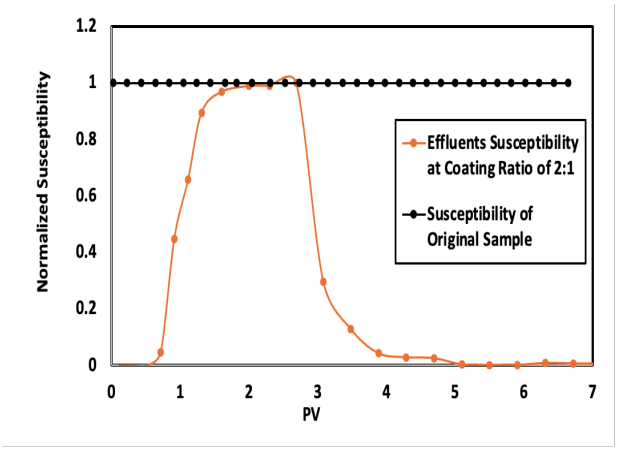

Fig. 12. Normalized susceptibility of the effluents as a function of PV for the flow test by injection of nanoemulsions with 2:1 polymer-to-nanoparticle ratio.

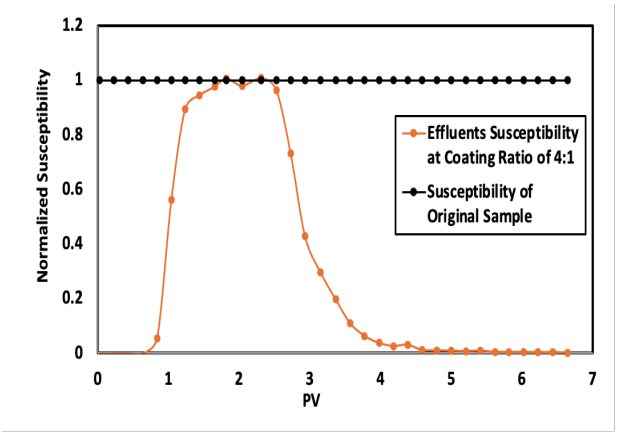

Fig. 13. Normalized susceptibility of the effluents as a function of PV for the flow test by injection of nanoemulsions with 4:1 polymer-to-nanoparticle ratio.

3.2.4 CT scanner utilization to monitor nanoemulsion dynamic transportation during nanoemulsion and chase water flooding

The CT scanner was used effectively to monitor nanoemulsion dynamic transportation through the sandpack by interpreting the obtained images. Figure 14 (a, b, and c) shows the apparent fluid density profiles obtained from CT scanning during nanoemulsion (NE) flooding at ratios of 0.5:1, 2:1, and 4:1, respectively. Similarly, Figure 15 presents the apparent fluid density profiles during subsequent chase water flooding, with (a) corresponding to the 0.5:1 ratio, (b) to the 2:1 ratio, and (c) to the 4:1 polymer-to-nanoparticle ratio. To enhance the contrast between the nanoemulsion and deionized (DI) water in the CT images—given their similar densities—2 wt.% of potassium iodide (KI) dopant was dissolved in the DI water. This addition increased the CT number of DI water, resulting in an apparent density increase of the water phase by 1300 g/cm³ as detected by the CT scanner. This method effectively distinguished between the nanoemulsion and the DI water, allowing for more accurate density measurements and improved visualization of fluid distribution within the porous media. From the results of Figure 14, nanoemulsion concentration increases by injecting nanoemulsion into the sandpack, the migration front distributes through the pores and penetrates deeper into the medium. These nanoemulsions move piston-like along the sandpack. Consequently, after 1.2 PV of nanoemulsion injection, the sandpack is fully saturated with nanoemulsion. The nanoemulsion (NE) flooding process was conducted up to 2 pore volumes (PV), followed by the injection of 5 PV of water to observe the displacement of the nanoemulsion by a less viscous liquid phase. In all polymer-to-nanoparticle ratios (4:1, 2:1, and 0.5:1), the sandpack became fully saturated with water after 1.2 PV of water injection. The subsequent chase water injection pushed the nanoemulsion slug toward the outlet of the sandpack. Due to the dilution effect caused by water, as noted by Boxin Ding et al. [22], the concentration of the trailing end of the nanoemulsion slug began to decrease.

Figures 14 (a), (b), and (c) illustrate that the water displacement by the nanoemulsion is comparable for all the ratios, with the sandpack achieving full saturation with nanoemulsion after the injection of 2 PV. Upon injecting 5 PV of water, the fluid phase density nearly returned to the initial water density, as shown in Figure 15 (c). This indicates that the 4:1 ratio nanoemulsion is stable enough to traverse the sandpack without significant retention of nanoparticles or oil droplets on the sand surfaces or within the pore throats. This stability is attributed to the negative charge of the silica sand and the similarly negative charge of the nanoemulsions stabilized with polymer coated nanoparticles (PIONP). The strong electrostatic repulsion between these negatively charged entities prevents the adsorption of nanodroplets onto the sand grain surfaces, aligning with the observed effluent density profile during chase water flooding. In contrast, Figure 15 (a) and (b) show that during water flooding in the experiments with the 0.5:1 and 2:1 ratios, while mobile nanodroplets were displaced through the sandpack and appeared in the

effluent, some immobile nanodroplets were uniformly trapped within the sandpack. This is evidenced by the difference between the apparent fluid density in the sandpack and the initial water density after injecting 5 PV of water. This suggests that the lower stability of the 0.5:1 and 2:1 ratios of nanoemulsion due to lower negative charge density around the nanoparticles results in oil droplets detaching from the nanoparticles and obstructing confined pore throats through bridging [23] or deposition mechanisms [24]. Despite the variation in the polymer-to-nanoparticle ratio from 4 to 0.5, there was no significant accumulation of nanoparticles observed in either experiment. Furthermore, by calculating the velocity of nanoparticles based on the breakthrough time of the nanoemulsion and the length of the sandpack, and comparing this velocity with the injection velocity, it is observed that they are approximately the same. This indicates that only minor heterogeneity is present through the sandpack. These findings highlight the importance of the nanoemulsion formulation in achieving efficient displacement and minimal retention within porous media. The stable 4:1 ratio formulation facilitates better displacement with reduced retention, whereas the less stable 0.5:1 ratio leads to partial blockage and retention due to the instability and detachment of oil droplets. This understanding is crucial for optimizing nanoemulsion systems for applications in fracture characterization, enhanced oil recovery, and other subsurface processes. [25].

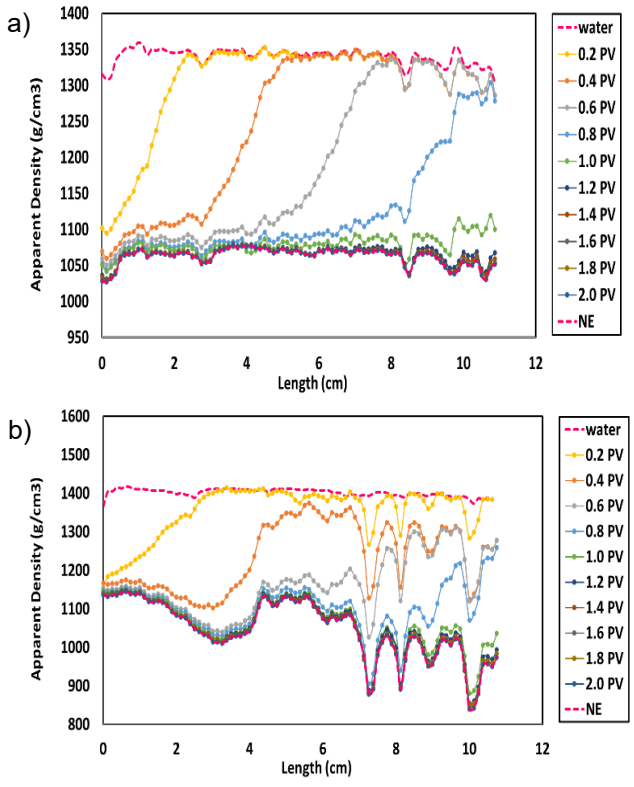

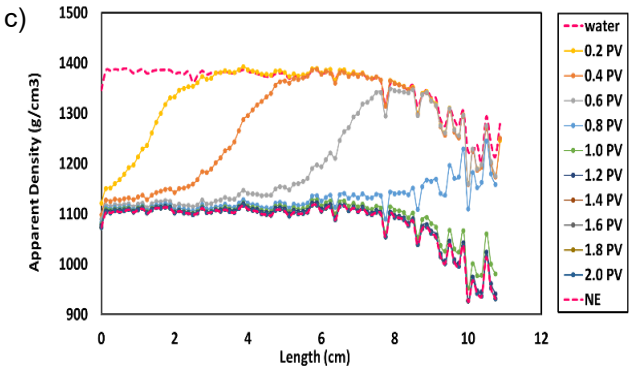

Fig. 14. Apparent fluid density profile during nanoemulsion flooding at the ratio of a) 0.5:1, b) 2:1, and c) 4:1.

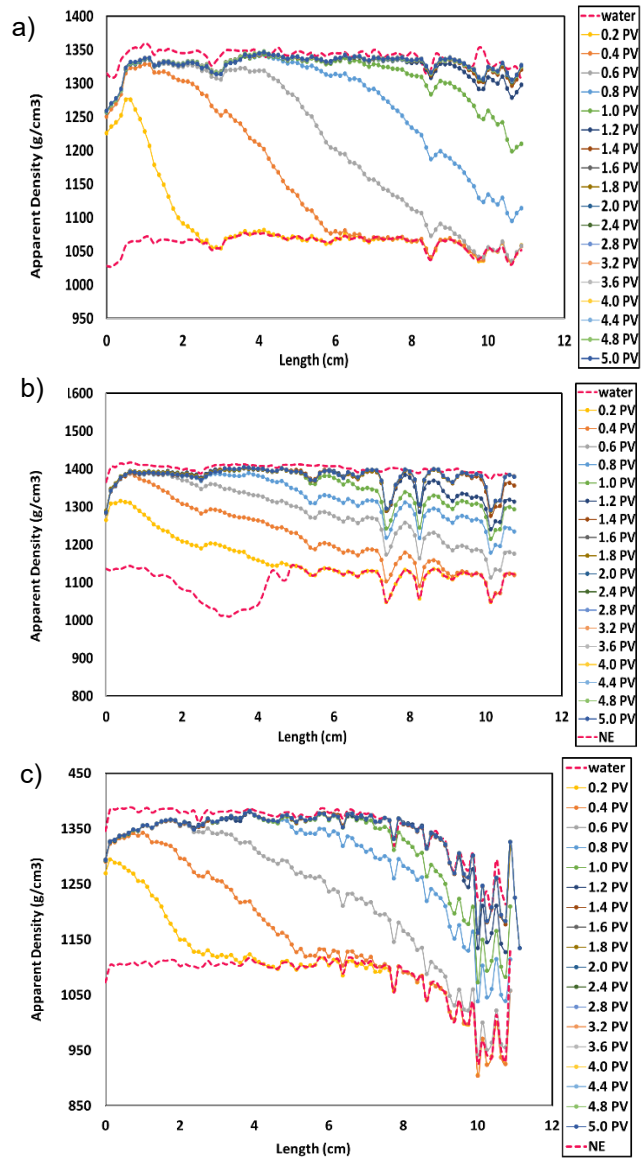

Fig. 15. Apparent fluid density profile during chase water flooding at the ratio of a) 0.5:1, b) 2:1, and c) 4:1.

4 Conclusion

The presented study investigates the magnetic nanodroplets propagation in porous media and offers valuable insights into the pressure drop, effluent droplet size distribution, concentration, and susceptibility profiles. The investigation, which explored different polymer-to-nanoparticle ratios (0.5:1, 2:1, and 4:1), elucidated how the stability of nanoemulsions affects their displacement and retention behaviors. The following conclusions were drawn from the variables examined:

- The observed pressure drop during nanoemulsion (NE) flooding, attributed to drag and viscous forces, is significantly higher compared to water flooding, indicating the influence of NE properties on flow behaviour in porous media. Additionally, it is evident that other phenomena, such as interfacial interactions and nanoparticle retention, also play a role in modulating the pressure drop behavior.
- The rate of pressure rise during NE flooding varies with the polymer-to-nanoparticle ratios, with higher ratios exhibiting less pronounced pressure increases, suggesting a relationship between NE stability and coating composition. To provide a more rigorous definition, NE stability refers to the ability of the nanoemulsion to maintain its dispersed state over time and under various environmental conditions, while coating composition pertains to the relative proportions of polymer and nanoparticles in the emulsion formulation. By increasing the coating thickness on the surface of nanoparticles, the stability of the nanoemulsion increases, and the retention of the nanoemulsion in porous media decreases.
- Effluent droplet size distribution analysis reveals that retention of PIONP-stabilized NE increases as the polymer-to-nanoparticle ratio decreases, leading to a reduction in median droplet size in effluent, particularly evident at lower coating ratios.
- ICP analysis demonstrates that as the polymer-to-nanoparticle ratio decreases, indicating polymer coating detachment and IONP deposition, greater retention of NE occurs during displacement experiments, highlighting the importance of coating ratio in NE stability and retention.
- Susceptibility measurements confirm the stability of synthesized Pickering NE during flooding experiments, with no observed retention or deposition, suggesting its potential as a displacement agent in porous media applications.
- The apparent fluid density profiles obtained from CT scanning demonstrate the uniform displacement of nanoemulsion at all polymer-to-nanoparticle ratios. During the experiment with a 4:1 ratio, the apparent density of the fluid phase in the sandpack nearly returns to the initial water density, indicating the stability of the nanoemulsion with minimal retention of nanoparticles or oil droplets. In contrast, a slight difference in the fluid density profile observed for the 0.5:1 ratio is attributed to phase separation within the nanoemulsion, which leads to less stable behavior. The phase separation causes oil droplets to detach from the nanoparticles, resulting in partial blockage and retention within the sandpack.

Overall, these findings confirm the critical role of polymer-to-nanoparticle ratio in governing NE stability, retention, and flow behavior in porous media, offering insights for optimizing NE formulations for enhanced displacement efficiency and reservoir management strategies.

The authors would like to acknowledge the generous financial support provided by the Canada First Research Excellence Fund (CFREF) Program, The Fundamentals of Unconventional Resources (FUR) Program (supported by NSERC, Alberta Innovates, Chevron, CNRL, ConocoPhillips, Enerplus), The Energi Simulation Industrial Research Chair in Energy Transition and the Canada Excellence Research Chair (CERC) Program for facilitating this research. Special recognition is extended to Brian Baillie from the CERC lab for his invaluable contribution to conducting ICP-MS tests.

Nomenclature

CT	Computed tomography
DI	Deionized Water
DLS	Dynamic Light Scattering
DP	Differential pressure between the inlet and outlet (psi)
EOR	Enhanced Oil Recovery
Fe_3O_4 NPs	Iron oxide nanoparticles
GE	General Electric
IONP	Iron oxide nanoparticles
ICP-MS	Inductively coupled plasma-mass spectrometry
KI	Potassium iodide
k	Permeability
M_w	Molecular weight
NE	Nanoemulsion
NP	Nanoparticle
nm	Nanometer
O/W	Oil-in-water
PV	Pore volume
PIONP	Polymer-coated Iron oxide nanoparticles
Q	Flow Rate
rpm	Revolutions per min
v/v%	Volume percentage
wt%	Weight percentage
Ø	Porosity

References

1. J. Zhang, Y. Miao, Z. Liu, & S. Yu, Adv. Colloid Interface Sci, **269**, 337-355, (2019).
2. H. Salehizadeh, & S. A. Shojaosadati, Water Res., **35(18)**, 4223-4228, (2001).

3. L. Zhang, S. Abdu, N. I. Khan, Y. Liang, & Y. Zhu, Energy Fuels, **33(3)**, 1953-1971, (2019).
4. H. Li, L. Wu, L. Cao, & Y. Zhang, Soft Matter, **15(6)**, 1144-1161, (2019).
5. Z. Li, C. Yang, S. Yang, J. Liu, Z. Zheng, C. Lu, & W. Li, Chem. Eng. J., **327**, 1041-1049, (2017).
6. B. Ding, S. H. Ahmadi, P. Babak, S. L. Bryant, A. Kantzas, Langmuir., **39, 20,** 6975-6991, (2023).
7. S. H. Ahmadi, B. Ding, S. L. Bryant, A. Kantzas, SPE, 212722-MS, (2023).
8. V. N. Burganos, E. D. Skouras, C. A. Paraskeva, A. C. Payatakes, AIChE Journal, **47**, 880-894, (2001).
9. S. P. Moulik, B. K. Paul, Adv. Colloid Interface Sci, (1998).
10. B. K. Paul, S.P. Moulik, Dispersion Sci. Technol., **18**, 301-67, (1997).
11. G. D'Avino, P.L. Maffettone, J. Non-Newtonian Fluid Mech., **215**, 80-104, (2015).
12. A. Perazzo, G. Tomaiuolo, V. Preziosi, S. Guido, Adv. Colloid Interface Sci, **256**, 305-325, (2018).
13. S. H. Ahmadi, S. Maaref, B. Ding, S. E. Siadatifar, D. Mayorga Ariza, S. L. Bryant, A. Kantzas, SPE, 218036-MS, (2024).
14. D. McAuliffe, SPE-4369-PA, 727-733, (1973).
15. R. Bulletin, AAPG Bulletin, **17**, 1521-26, (1933).
16. L. Yu, M. Dong, B. Ding, Y. Yuan, Chem. Eng. Sci., **178**, 335-347, (2018).
17. Cao, Changqian, E. Abdelphata, A. Meimanova, J. Wang, J. Yu, P. Gong, J. Zhao, Y Zhang, F. Fang, A. Kantzas, M. Trifkovic, S. Bryant, Y. Pan, *Physical Sciences*, (2021).
18. B. Ding, S. L. Bryant, A. Kantzas, *Patent Application Publication,* (2023)
19. Shanmugam, Akalya, M. Ashokkumar, Food Hydrocoll., 39, 151-62, (2014).
20. N. R. Morrow, J. Pet. Technol., **27(08)**, 937-947, (1975).
21. J. Foroozesh, S. Kumar, Mater. Lett., **316**, 113876, (2020).
22. B. Ding, Q. Sang, Z. Nnie, Z. Li, M. Dong, Z. Chen, A. Kantzas, SPE Journal, **26 (5)**, 3094-3108, (2021).
23. Yao, Chuanjin, B. Liu, L. Li, K. Zhang, G. Lei, T. S. Steenhuis. Environ. Sci. Technol., **54 (17)**, 10876–84, (2020).
24. Yu, L, B Ding, M Dong, Q Jiang, ACS Publications, 57 (43), 14795-808, (2018).
25. S. H. Ahmadi, S. Maaref, B. Ding, S. E. Siadatifar, D. Mayorga Ariza, S. L. Bryant, A. Kantzas, SPE-218036-MS, (2024).

APPENDIX: Emulsion Stability Definitions

The term "stability" of nanoemulsions refers to the ability of the nanoemulsion system to maintain its properties and structure over time without undergoing significant changes or separation. Stability in the context of nanoemulsions can be assessed in several ways:

Thermodynamic Stability:

Phase Separation: A stable nanoemulsion should resist phase separation, where the dispersed droplets (e.g., oil droplets in an oil-in-water nanoemulsion) do not coalesce and separate from the continuous phase (e.g., water).

Aggregation and Coalescence: Stability implies that the nano-sized droplets do not aggregate or coalesce into larger droplets over time, maintaining their small size and uniform distribution.

Kinetic Stability:

Sedimentation and Creaming: Due to the small size of the droplets, a stable nanoemulsion should exhibit minimal sedimentation (settling of droplets under gravity) or creaming (rising of droplets to the top). The Brownian motion should counteract these tendencies.

Ostwald Ripening: A stable nanoemulsion should be resistant to Ostwald ripening, a process where smaller droplets dissolve and redeposit onto larger droplets, causing changes in droplet size distribution over time.

Chemical Stability:

Oxidation and Degradation: The components of the nanoemulsion, such as oils, surfactants, and any active ingredients, should resist chemical degradation, oxidation, or hydrolysis over the desired shelf life.

Physical Stability:

Temperature and pH Variations: A stable nanoemulsion should withstand changes in environmental conditions like temperature fluctuations and pH changes without breaking down or altering its properties significantly.

Mechanical Stability:

Shear and Stress: Nanoemulsions often need to be stable under mechanical forces such as shear stress from mixing or pumping. Stability implies that the emulsion does not break or separate under such conditions.

The stability of nanoemulsions encompasses a broad range of characteristics ensuring that the emulsion remains homogeneous, with uniformly dispersed nano-sized droplets, and retains its functional properties over a specified period and under expected conditions of use.